CORROSION SCIENCE AND TECHNOLOGY, Vol.18, No.6(2019), pp.232~242
[Research Paper]
pISSN: 1598-6462 / eISSN: 2288-6524
DOI: https://doi.org/10.14773/cst.2019.18.6.232

Analysis of PVDF Coating Properties with Addition of Hydrophobically Modified Fumed Silica

Nam Kyu Lee, Young Hoon Kim, Tae Gyu Im, Dong Uk Lee, MinYoung Shon, and Myung Jun Moon†

Department of Industrial Chemistry, Pukyong National University, Busan, 48547, Republic of Korea

(Received October 25, 2019; Revised November 25, 2019; Accepted November 25, 2019)

In this study, hydrophobically modified fumed silica was added to the PVDF coating to improve corrosion protection performance. Two types of silane modifiers, trimethylchlorosilane (TMCS) and hexamethyldisilazane (HMDZ), were used for hydrophobic modification of the fumed silica. The composition of modified fumed silica was analyzed by Fourier transform infrared, X-ray photoelectron spectroscopy, and elemental analysis. The dispersion of modified fumed silica in the PVDF coating was observed by the transmission electron microscopy, and the hydrophobicity of PVDF coating was analyzed by the water contact angle. Surface properties were examined by the field emission scanning electron microscopy and scanning probe microscopy. Potentiodynamic polarization was conducted to confirm corrosion protection performance of PVDF coating in terms of hydrophobically-modified fumed silica contents. As a result, the average surface roughness and the water contact angle of the PVDF coating increased with modifier contents. The results of the potentiodynamic polarization test showed an increase of the E_{corr} values with increase of the hydrophobicity of PVDF coating. Thus, it clearly indicates that the corrosion protection performance of PVDF coating improved with the addition of the hydrophobic-modified fumed silica that prevents the penetration of moisture into the PVDF coating.

Keywords: *Polyvinylidene fluoride, Hydrophobic modification, Fumed silica*

1. Introduction

In recent years, super-hydrophobic coatings have attracted attention in many fields because they have unique characteristics such as anti-sticking, anti-icing, anti-contamination, anti-corrosion and self-cleaning [1-5]. Surface with a contact angle higher than 150 degrees between water and the surface is called superhydrophobic surfaces. A representative example of a superhydrophobic surface present in nature is a lotus. In 1997, German botanists W. Barthlott and C. Neinhuis studied the surface structure of lotus. The surface of the petal was found to be covered with a low surface energy material and had a complex surface roughness of nano and micro size [2]. Since then, many researchers have been studying to fabricate a rough surface on a material with low surface energy or surface modification of a rough surface with low surface energy to realize an artificial superhydrophobic coating.

Various fluoropolymers are mainly used to make hydrophobic coatings. These coatings contain fluorine in the polymer chain and have unique properties such as heat resistance, chemical resistance, stain resistance and low surface energy compared to other hydrocarbon polymers [19,20].

Polyvinylidene fluoride (PVDF) is mainly used fluoropolymer coating material, because of comparatively excellent compatibility with solvents, low surface energy (25 dynes/cm), excellent mechanical strength, thermal stability, weather ability and chemical resistance [9,12].

Various studies have been conducted to make superhydrophobic coatings by adding various pigments such as fumed silica to PVDF coatings [4-11]. Fumed silica has hydrophilic properties because it has many hydroxyl groups on the surface. Thus, if fumed silica is added as a pigment without any treatment, it is easily agglomerated and difficult to obtain good dispersion in the coating [13]. To solve these problems, the hydrophobic surface modification of fumed silica has been used to improve the dispersibility [4].

Recently, the use of commercial hydrophobic fumed silica was available and it must be added more than 70 wt% of the resin to make hydrophobic coating. In the present study, a new modification process of the fumed silica was carried out using two modifiers, trimethyl-

†Corresponding author: mjmoon@pknu.ac.kr

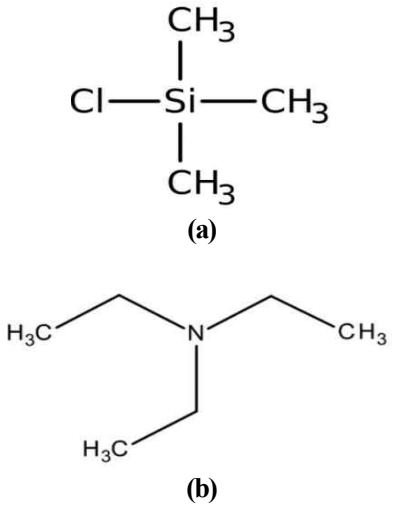

Fig. 1 Chemical structure of materials during modification process. (a) TMCS, (b) TEA

chlorosilane (TMCS) and hexamethyldisilazane (HMDZ) to achieve hydrophobic property. Then, the corrosion protection performance of PVDF coatings with fumed silica modified with TMCS and HMDZ was compared to that of PVDF coatings with commercial fumed silica.

2. Experimental Methods

2.1. Materials

For hydrophobic surface modification, trimethylchlorosilane (TMCS, Tokyo chemical industry, Japan) and hexamethyldisilazane (HMDZ, Tokyo chemical industry, Japan) were used as surface modifiers for fumed silica (Sigma-Aldrich, U.S.). Triethylamine (TEA, Junsei chemical, Japan) and trifluoroacetic acid (TFA, Daejung chemical, Korea) were used as catalysts and n-hexane (Daejung chemical, Korea) and ethyl alcohol (EtOH, Daejung chemical, Korea) were used as solvents. The PVDF coating solution was prepared by using PVDF powder (Sigma-Aldrich, U.S.) and N, N-dimethylformamide (DMF, Junsei chemical, Japan). The hot-rolled steel sheets were used as substrate materials for coating. The surface of steel sheets was blasted using 2 μm size of aluminum oxide, washed with acetone (Daejung chemical, Korea), and then coated with a one-component polyurethane primer. (PPG, Korea).

2.2. Surface modification of Fumed silica

2.2.1. Heat treatment of fumed silica

To improve the surface modification efficiency of fumed silica, heat treatment was carried out before modification [15]. The heat treatment was conducted to remove the adsorbed water on the surface of fumed silica and in order to reduce the ratio of hydrogen-bonded hydroxyl groups not involved in the reaction. It also increases the proportion of free hydroxyl groups, resulting in improving the efficiency of the modification [15]. In the present study, fumed silica was heated to 800 °C for 4 hours with a heating rate of 10 °C/min by a furnace (AJ-SB1, Ajeon Heating Industrial, Korea)

2.2.2. The hydrophobic surface modification of fumed silica using TMCS

The chemical structure of TMCS and TEA for surface modification are shown in Fig. 1. In surface modification process, 10 g of fumed silica was put into the 1 liter of n-hexane, followed by stirring at 60 °C and 25 ml of TEA was added as a catalyst, then TMCS was added 10, 30, 50, 70 and 80 wt% of the weight of fumed silica, respectively. After stirring at 60 °C for 12 hours, the aspiration process was carried out using n-hexane and EtOH to remove unreacted materials then dried at 60 °C for 12 hours. The dried modified fumed silica was stored after grinding. Fig. 2 shows the reaction mechanism.

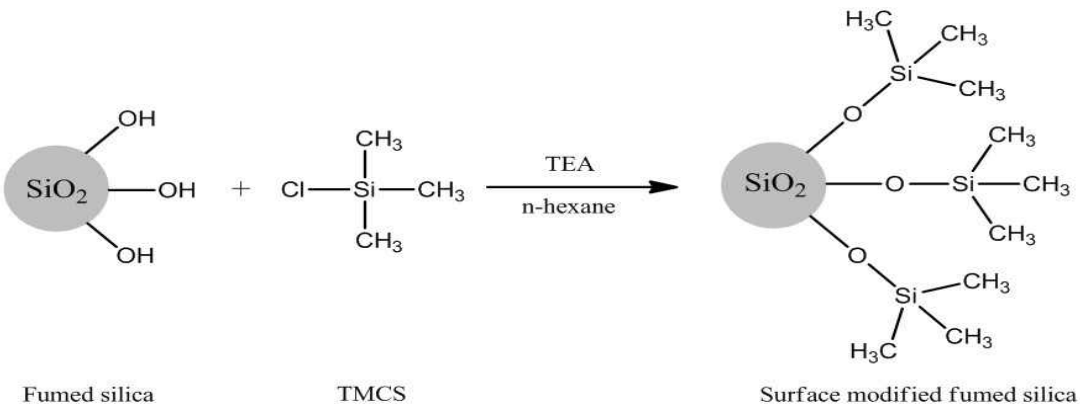

Fig. 2 Chemical reaction mechanism of fumed silica and TMCS.

2.2.3. hydrophobic surface modification of fumed silica using HMDZ

The chemical structure of HMDZ and TFA for surface modification is shown in Fig. 3. In surface modification process, 10 g of fumed silica was put into the 1 liter of n-hexane, followed by stirring at 60 ℃ and 3 ml of TFA was added as a catalyst, then HMDZ was added 10, 30, 50, 70 and 80 wt% of the weight of fumed silica, respectively. The aspiration process was carried out using n-hexane and EtOH to remove unreacted materials then dried at 60 ℃ for 12 hours. The dried modified fumed silica was stored after grinding. Fig. 4 shows the reaction mechanism and Table 1 shows the sample names and synthesis conditions.

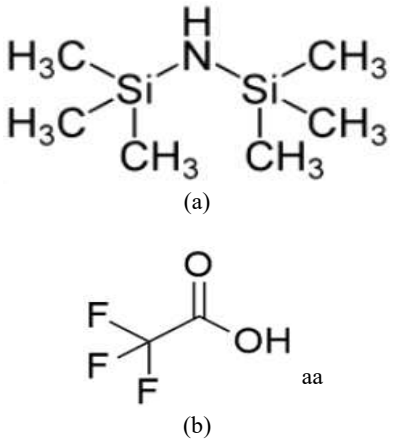

Fig. 3 Chemical structure of materials during the modification process. (a) HMDZ, (b) TFA

2.3. Manufacture of PVDF coating solution with hydrophobically modified fumed silica

The 7 wt% of the PVDF solution was prepared by dissolving PVDF powder in DMF and stirring at 50 ℃ until the solution becomes transparent. After that, the 7 wt% of PVDF solution and modified fumed silica were mixed with a weight ratio of 1:1 and the PVDF solution was stirred and sonicated at room temperature for 1 hour until it becomes transparent. Also, in the same process

Table 1 The sample name and modification conditions

Sample	Solvent	Modifier	Synthesis time	Concentration(wt%)
S	-	-	-	-
T10	n-hexane	TMCS	12h	10
T30				30
T50				50
T70				70
T80				80
H10	n-hexane	HMDZ	12h	10
H30				30
H50				50
H70				70
H80				80

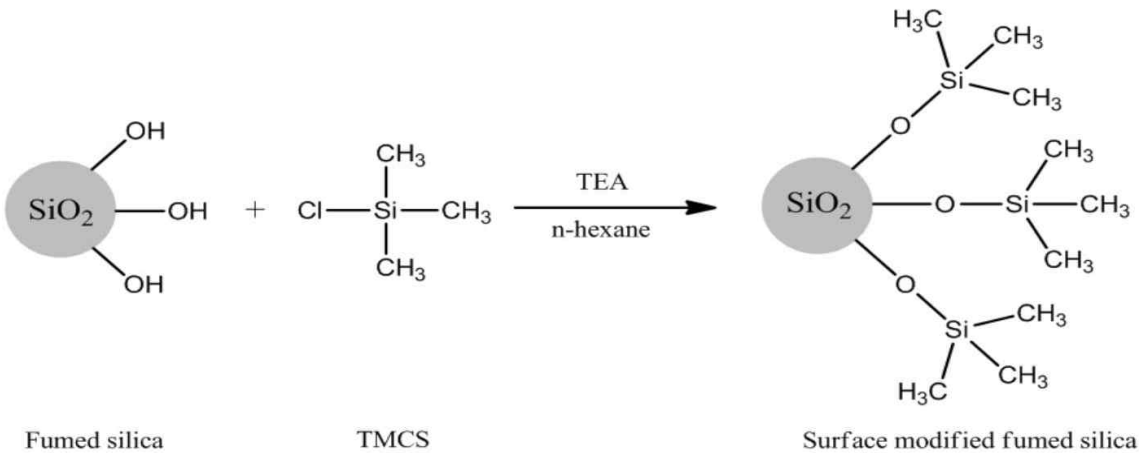

Fig. 4 Chemical reaction mechanism of fumed silica and HMDZ.

Table 2 The name of the coated sample according to the type of fumed silica

Sample	Resin	Type of fumed silica	Coating method
P0	PVDF		Spray coat
PT10		T10	
PT30		T30	
PT50		T50	
PT70		T70	
PT80		T80	
PH10		H10	
PH30		H30	
PH50		H50	
PH70		H70	
PH80		H80	
PR816		AEROSIL® R816	Bar coat
PR976		AEROSIL® R976	

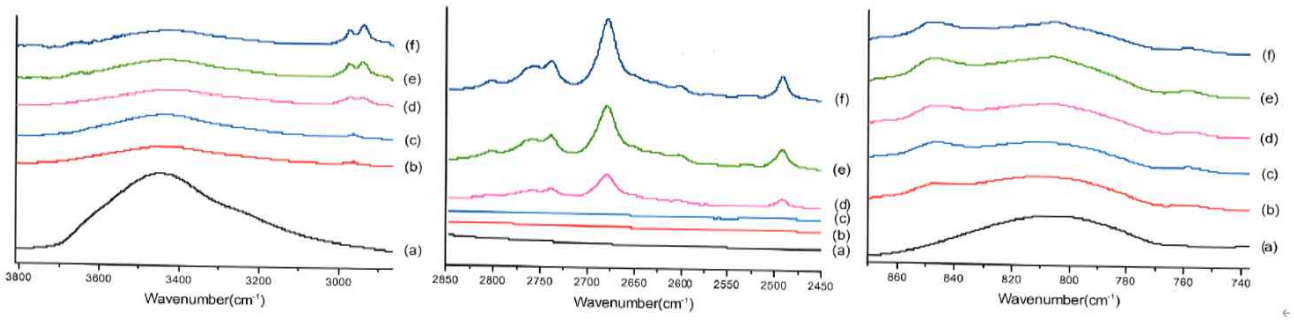

Fig. 5 FT-IR spectrum according to the amount of TMCS. NS, (b) T10, (c) T30, (d) T50, (e) T70, and (f) T80

as above, PVDF solutions were prepared with the addition of commercial hydrophobic fumed silica, AEROSIL® R816 (Evonik) and AEROSIL® R976 (Evonik).

2.4. Specimens fabrication and coating treatment

The hot-rolled steel sheet was blasted with 2 μm size of aluminum oxide and washed with acetone for 10 minutes in the ultrasonic cleaner. Urethane primer was applied to the blasted specimen using a no. 24 bar coater and cured at 300 °C for 5 minutes, then PVDF coating was sprayed and cured at 110 °C for 4 hours. The dry coating film thickness was 21 ± 2 μm. Table 2 shows the names of specimens according to the types of fumed silica in the PVDF coating.

2.5. Analysis

FT-IR (Fourier transform infrared, Nicolet iS10, Thermoscientific U.S.A.) was used to analyze the chemical functional group of the surface-modified fumed silica. XPS (X-ray photoelectron spectroscopy, MultiLab2000, 0.5 eV Al Kα, Thermo VG Scientific, U.K.) and EA (Elemental analysis, Leco Truspec Micro, U.S.A.) were used to analyze surface material composition changes of the surface-modified fumed silica. The dispersion of fumed silica in toluene was observed by TEM (Transmission Electron Microscopy, Tungsten Filament type, HITACHI H-7500, Japan). For TEM analysis, 0.1 wt% of fumed silica was dispersed in 20 g of toluene by sonication and stirring. The hydrophobicity of the coatings according to the surface modification of fumed silica, was analyzed using the water contact angle measurement (SEO Pheonix150, Korea). The surfaces of PVDF coatings were observed using FE-SEM (TESCAN MIRA 3 LMH In-Beam, Czech). The surface roughness of PVDF coating with the contents of fumed silica was measured by scanning probe microscopy (BRUKER Icon-PT-PLUS, USA). Potentiodynamic polarization analysis was performed to evaluate the corrosion protection performance using PARSTAT 2273 (EG&G Princeton applied research, U.S.A.)

3. Results

3.1. Analysis of fumed silica

3.1.1. Fourier transform infrared spectroscopy (FT-IR)

Fig. 5 shows the FT-IR spectrum of 3800 ~ 2860 cm^{-1} and 870 ~ 740 cm^{-1} region depending on the amount of

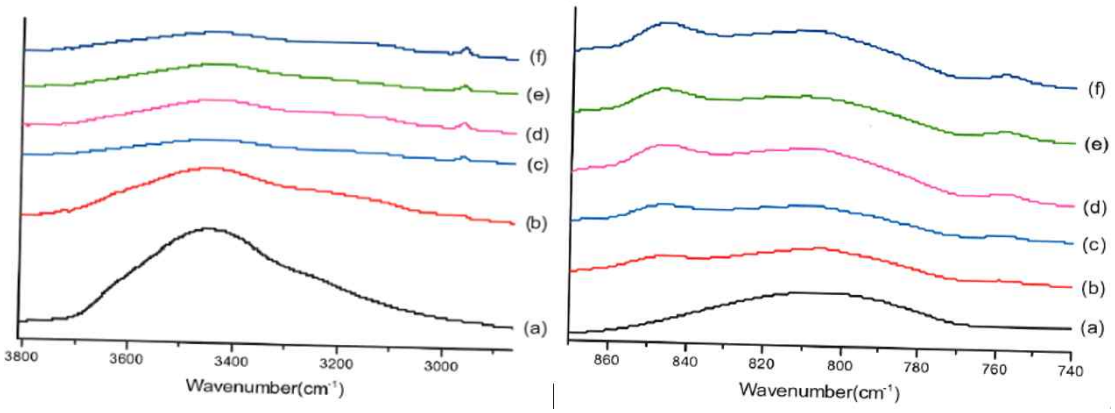

Fig. 6 FT-IR spectrum according to the amount of HMDZ. (a) NS, (b) H10, (c) H30, (d) H50, (e) H70, and (f) H80

Table 3 Elemental analysis of unmodified and modified fumed silica

Sample	C %/mg	H %/mg	N %/mg
NS	0.655069	0.409446	0.3328
T10	1962482	0.85581	1.0341
T30	2.006774	0.951828	1.9433
T50	5805325	0.979675	2.4717
T70	7.743762	1.183836	3.2274
T80	9.365313	1525719	3.0425
H10	3.090976	0.773244	0.539
H30	4.841998	0.909682	1.5841
H50	4.883243	0.733199	1.0487
H70	6.21812	1.126786	0.0686
H80	8.544563	1.490909	0.7176

TMCS, and Fig. 6 shows the FT-IR spectrum of 3800 ~ 2860 cm^{-1} and 870 ~ 740 cm^{-1}, depending on the amount of HMDZ.

3.1.2. X-ray photoelectron spectroscopy (XPS)

The surface composition of fumed silica was analyzed by X-ray photoelectron spectroscopy (XPS) Si2p spectrum with an increasing amount of modifier during the modification process. The results are shown in Fig. 7, Fig. 8, and Fig. 9.

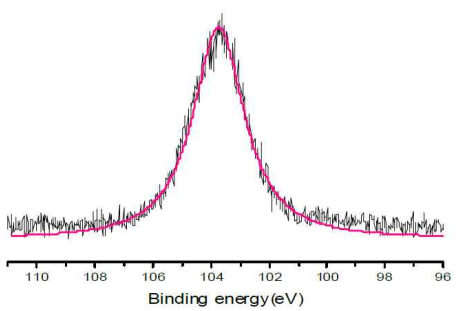

Fig. 7 Si 2p spectrum of NS.

3.1.3. Elemental analysis (EA)

To analyze the change of the surface carbon content of modified fumed silica depending on the contents of the modifier, elemental analysis (EA) was analyzed, and the results are shown in Table 3.

3.1.4. Transmission electron microscopy (TEM)

The dispersion of fumed silica was observed using Transmission electron microscopy (TEM) and the surface-modified fumed silica and unmodified fumed silica were observed at 100-fold magnification as shown in Fig. 10.

3.2. PVDF coating analysis with hydrophobic surface-modified fumed silica

3.2.1. Scanning probe microscopy (SPM)

The surface roughness of PVDF coating containing fumed silica was measured by SPM in terms of modifier contents.

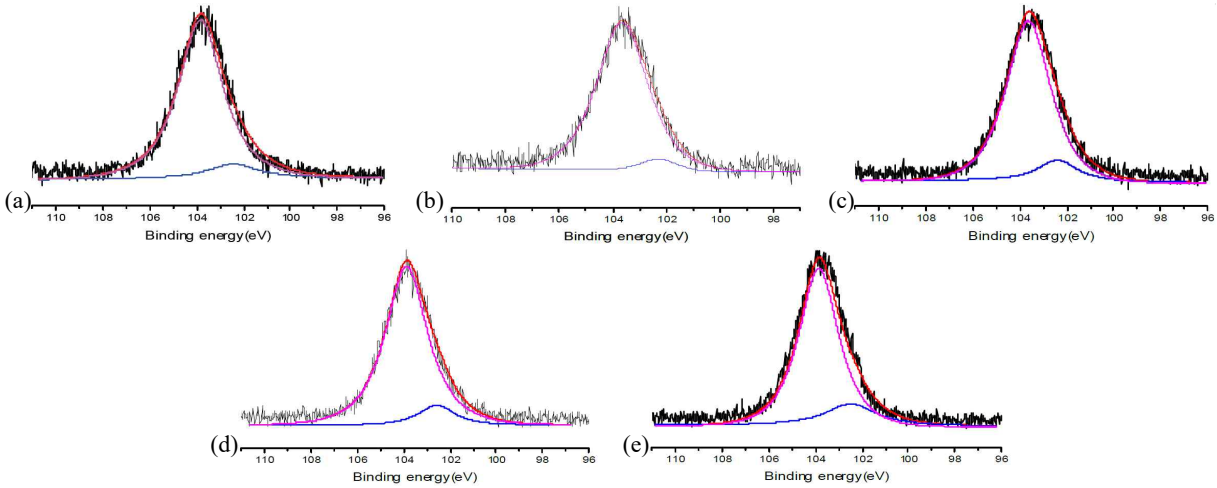

Fig. 8 Si 2p spectrum of modified fumed silica with TMCS. (a) T10, (b) T30, (c) T50, (d) T70, and (e) T80

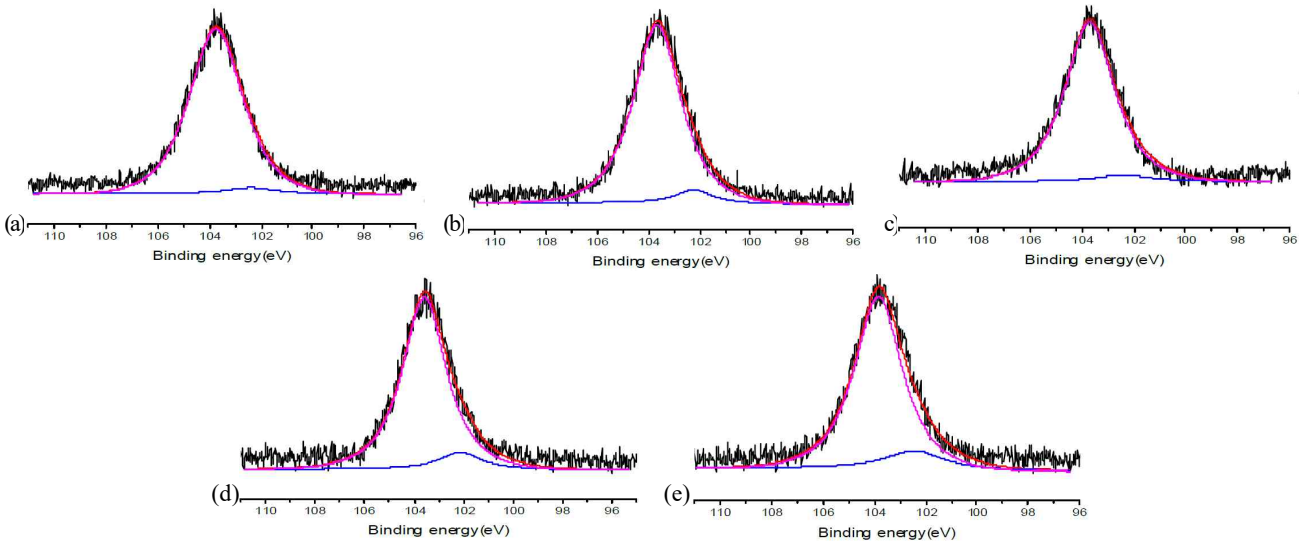

Fig. 9 Si 2p spectrum of modified fumed silica with HMDZ. (a) H10, (b) H30, (c) H50, (e) H70, and (e) H80

Table 4 The average surface roughness of PVDF coating with fumed silica

Sample	Average surface roughness (nm, R_a)
P0	21.8
PT10	36.3
PT30	41.2
PT50	41.8
PT70	43.4
PT80	44.1
PH10	35.1
PH30	40.3
PH50	44.1
PH70	50.7
PH80	56.4

Table 5 Water contact angle measurement of specimens

Sample	Average contact angle (°)
P0	75.88
PT10	104.59
PT30	145.48
PT50	85.87
PT70	87.51
PT80	88.77
PH10	95.17
PH30	137.74
PH50	140.43
PH70	150.00
PH80	151.92

The average roughness (Ra) of each specimen is shown in Table 4.

3.2.2. Water contact angle (WCA)

To confirm the relationship between surface roughness of the coating and hydrophobicity, the contact angle measurement was conducted according to the type and adding contents of the modifier and the results were listed in Table 5.

3.2.3. Field emission scanning electron microscopy (FE-SEM)

The surface morphology of fumed silica in PVDF coating was observed by FE-SEM at a magnification of 150,000 times. The SEM images were shown in Fig. 11 and Fig. 12.

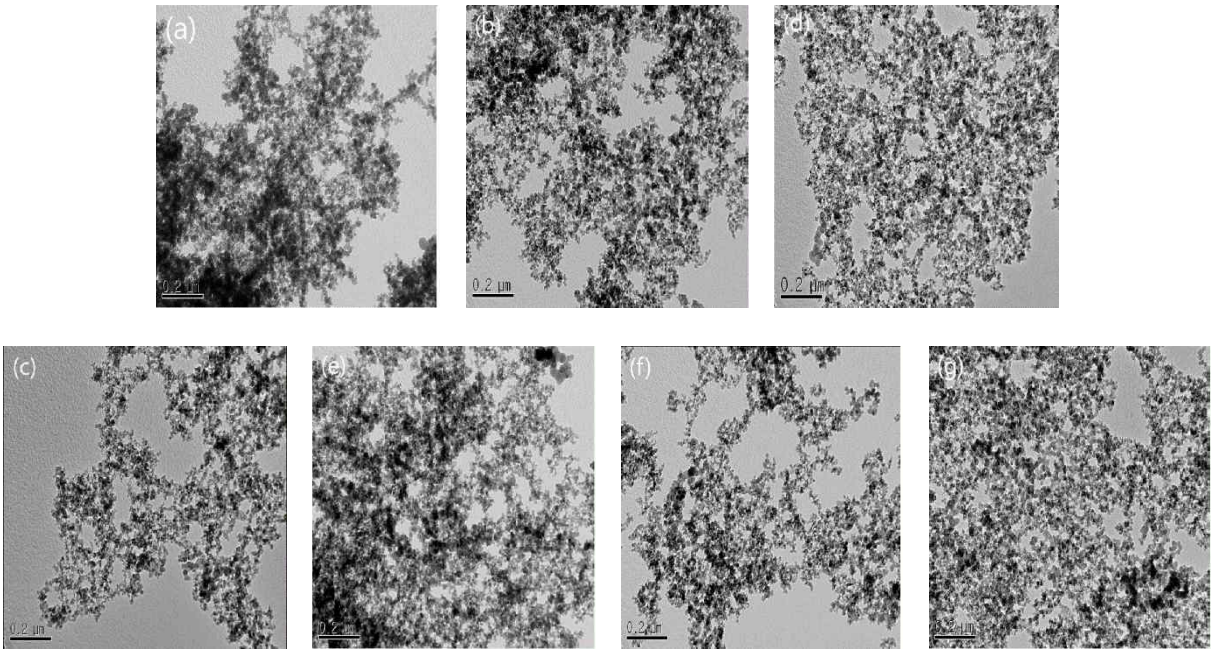

Fig. 10 B-TEM images of fumed silica. NS, (b) T10, (c) T50, (d) T80, (e) H10, (f) H50, and (g) H80

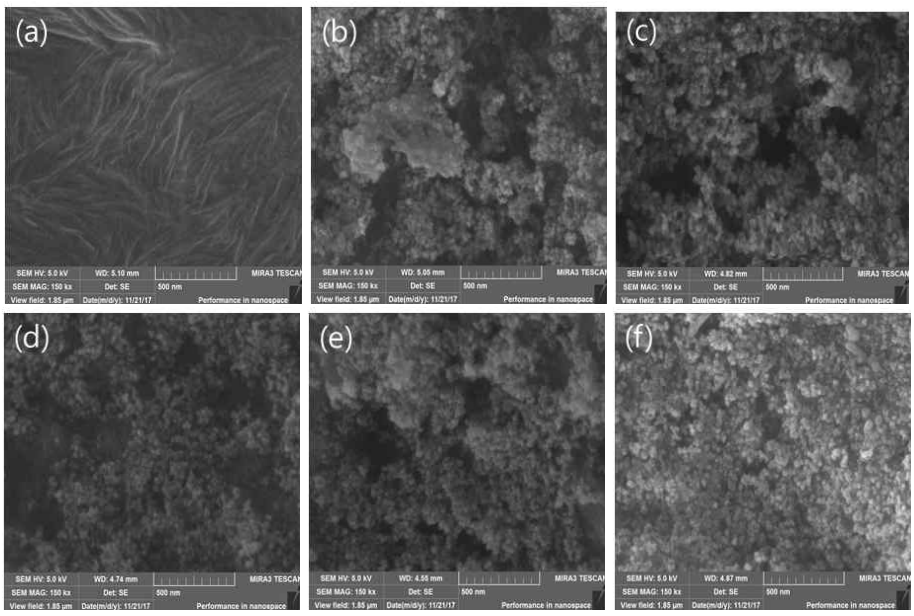

Fig. 11 SEM images of surface morphology of PVDF coatings with TMCS. (a) P0, (b) PT10, (c) PT30, (d) PT50, (e) PT70, and (f) PT80

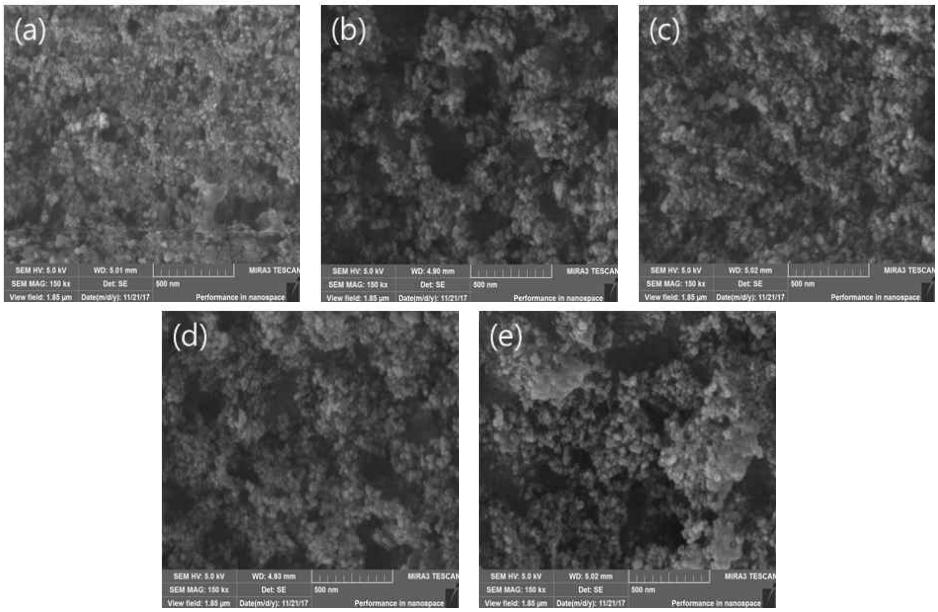

Fig. 12 SEM images of surface morphology of PVDF coatings with HMDZ. (a) PH10, (b) PH30, (c) PH50, (d) PH70, and (e) PH80

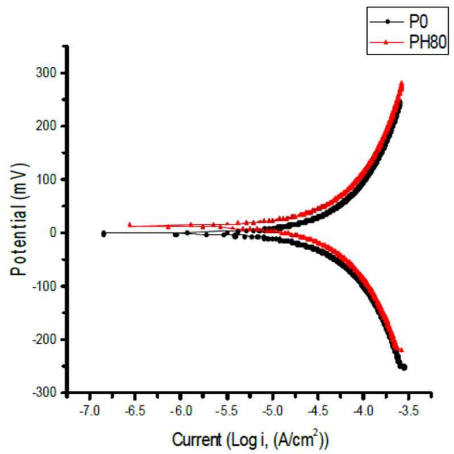

Fig. 13 Potentiodynamic polarization curve of P0 and PH80.

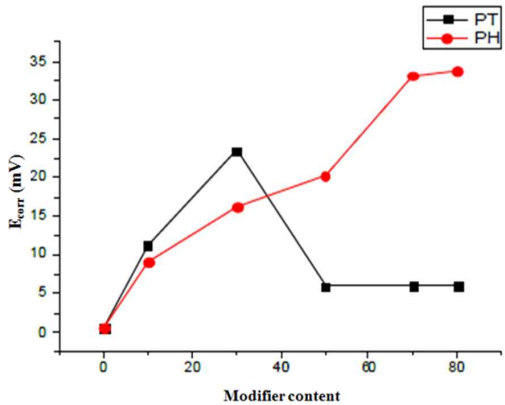

Fig. 14 Ecorr variation of specimens.

3.2.4. Potentiodynamic polarization test

The potentiodynamic polarization test was carried out in 0.35 wt% NaCl solution to evaluate the corrosion protection performance of the specimens. The potentiodynamic polarization curves of PH80 (the highest hydrophobic property) and P0 (the lowest hydrophobic property) were shown in Fig. 13. The variations of E_{corr} and I_{corr} of the specimens were described in Fig. 14 and Fig. 15, respectively. The polarization curve of PR816, PR976

Table 6 Ecorr and Icorr of specimens

Sample	E_{corr} (mV)	I_{corr} (A/cm^2)
P0	0.586	15.16×10^{-5}
PT10	11.218	11.19×10^{-5}
PT30	23.492	3.11×10^{-5}
PT50	5.924	15.02×10^{-5}
PT70	6.014	14.81×10^{-5}
PT80	6.032	14.73×10^{-5}
PH10	9.127	12.76×10^{-5}
PH30	16.187	7.45×10^{-5}
PH50	20.326	5.98×10^{-5}
PH70	33.153	1.74×10^{-5}
PH80	33.726	1.41×10^{-5}
PR816	5.984	15.06×10^{-5}
PR976	6.053	13.21×10^{-5}

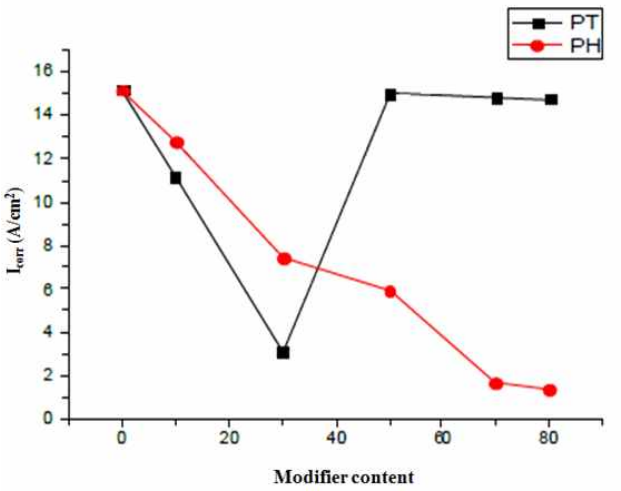

Fig. 15 Icorr variation of specimens.

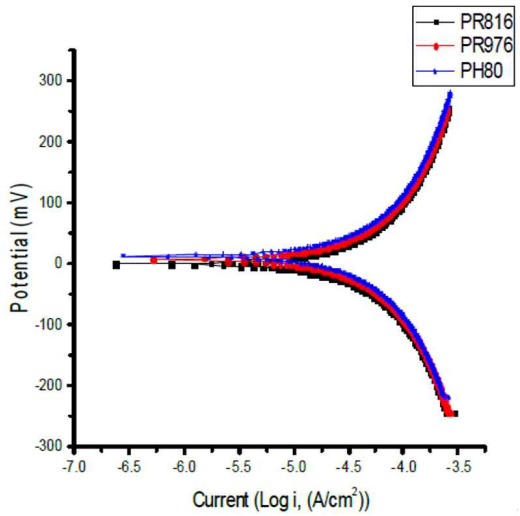

Fig. 16 Potentiodynamic polarization curve of PR816, PR976 and PH80.

and PH80 was shown in Fig. 16 and E_{corr} and I_{corr} values for all specimens were listed in Table 6.

4. Discussion

4.1. Analysis of fumed silica

4.1.1. Fourier transform infrared spectroscopy (FT-IR)

In Fig. 5, a large O-H absorption peak at 3450 cm^{-1}, indicating the hydroxyl group was shown in fumed silica without modification. After surface modification of fumed silica, the O-H absorption peak decreased and the aliphatic asymmetry absorption peak of a methyl group at 2971 cm^{-1} and the absorption peak of the trimethylsilyl group at 846 cm^{-1} increased with the increase of TMCS contents. Therefore, it was confirmed that the hydroxyl group decreased and replaced by the trimethylsilyl group of TMCS.

Table 7 Quantitative analysis of TMCS for modified fumed silica

	Methyl/hydroxyl	Trimethylsilyl/hydroxyl
NS	0	0
T10	0.15827	0.23741
T30	0.17919	0.26590
T50	0.19835	0.42975
T70	0.35333	0.47333
T80	0.51145	0.49802

Table 8 Quantitative analysis of HMDZ for modified fumed silica

	Methyl/hydroxyl	Trimethylsilyl/hydroxyl
NS	0	0
H10	0.0507	0.11149
H30	0.2155	0.40519
H50	0.2440	0.4881
H70	0.2516	0.5226
H80	0.952	0.77419

However, it can be confirmed that new absorption peaks are generated between the regions of 2850 to 2450 cm^{-1} of the modified fumed silica with 50 wt% or higher contents of TMCS, indicating the presence of triethylammonium chloride during the modification process [16]. From the results of FT-IR analysis, it can be seen that the reaction of the hydroxyl group and TMCS on the surface of fumed silica increases as the content of TMCS increases.

Table 7 and Table 8 show the ratio of the FT-IR peak intensity between the methyl group, trimethylsilyl groups and hydroxyl groups when fumed silica was modified with TMCS and HMDZ, respectively.

As the contents of HMDZ increases during the modification, the O-H absorption peak decreased. On the other hand, the intensity of the methyl group and the trimethylsilyl group increases. As a result of the FT-IR analysis, the hydroxyl groups of fumed silica act as reaction cites during the modification process and consequently became fumed silica more hydrophobic.

4.1.2. X-ray photoelectron spectroscopy (XPS)

In the XPS analysis of the Si 2p spectrum, the peak at 103.5 eV (Si- O_2 bond) and 102.1 eV(Si-C bond) were observed, as shown in Fig. 7, Fig. 8 and Fig. 9. in terms of contents of TMCS and HMDZ, respectively.

From the results, it was clearly demonstrated that the SiO_2 peak (103.5 eV) and Si-C peak (102.1 eV) were

increased with the increase of TMCS and HMDZ increase, respectively.

4.1.3. Elemental analysis (EA)

As described in Table 3 of EA analysis results, carbon contents of fumed silica surface increased with an increase of the modifier contents, indicating the increase of trimethylsilyl groups with high carbon content instead of hydroxyl groups. These results agreed well with FT-IR and XPS analysis results.

4.1.4. Transmission electron microscopy (TEM)

Fig. 10 shows the results of TEM observation. NS (Fumed silica, which is not treated with a modifier) is not distributed well due to its aggregation in solvents, whereas surface-treated fumed silica can be found to be well-dispersed. As a result, the use of surface-modified fumed silica to PVDF coating is considered to achieve uniform distribution in PVDF coating and hydrophobic surface properties.

4.2. Analysis of PVDF coating with hydrophobic surface-modified fumed silica

4.2.1. Scanning probe microscopy (SPM) and Water contact angle (WCA)

The surface roughness of PVDF coating increase with the increase of the modifier contents as described in Table 4 and the main cause of surface roughness increase seems caused by uniform dispersion and the increase of volume of fumed silica due to modification of TMCS and HMDZ as shown in Fig. 2 and Fig. 4.

Table. 5 shows the results of contact angle measurement according to the modifier contents. In case of PVDF coating with the TMCS modifier, the water contact angle increased with the increase of the TMCS modifier to 30 wt% then decreased to 88.77°. This Phenomenon seems caused by triethylammonium chloride, a kind of the water soluble hydrophilic salts. The triethylammonium chloride was formed on the fumed silica surface during the surface modification process when the TMCS more than 30 wt% was added to fumed silica. And it provided the water affinity to the PVDF coating [18]. On the other hand, the water contact angle of PVDF coating with the HMDZ modifier increase with the increase of the modifier contents.

4.2.2. Field emission scanning electron microscopy (FE-SEM)

PVDF coating surface was observed by SEM as shown in Fig. 11 and Fig. 12. In case of PVDF coating with TMCS modified fumed silica, the surface of the PVDF coating with higher contents of TMCS modified fumed silica was more porous and rough and this phenomenon was happened the PVDF coating with HMDZ modified fumed silica. This SEM observation result was agreed well to the results of scanning probe microscopy observation.

4.2.3. Potentiodynamic polarization test

Fig. 14, Fig. 15 and Table 6 show the potentiodynamic polarization test results of PVDF coatings in terms of modified fumed silica contents. From the results, E_{corr} values increased and the I_{corr} values decreased with the increase of HMDZ modified fume silica contents. These results clearly indicated that the corrosion resistance of the PVDF coating increased with the increase of hydrophobic property by the introduction of HMDZ modified fume silica. The improvement of corrosion protection seems caused by improving the barrier property against water penetration into coating [14]. However, PVDF coating with TMCS modified fumed silica show different tendency from that with HMDZ modified fume silica. The E_{corr} and I_{corr} values of PT50, PT70 and PT80 were lower than those of PT10 and PT30 and it because of the formation of hydrophilic triethylammonium chloride salts. These results are in good agreement with the results of the water contact angle of PVDF coating with TMCS that water contact angle increased with the increase of the TMCS modifier to 30 wt% then decrease to 88.77o. The corrosion protection performance of PVDF coating (PR816 and PR976) with commercial fumed silica was also compared with PVDF coating (PH80). Consequently, E_{corr} value of PH80 is significantly higher than that of PR816 and PR976.

5. Conclusion

In this study, the hydrophobically surface-modified fumed silica was synthesized and added to the PVDF coating. Surface modification of fumed silica was analyzed by FT-IR, XPS and EA and dispersion of modified fumed silica was observed by TEM analysis. Surface roughness and morphology of PVDF coating with modified fumed silica was examined by SPM and SEM observation. Finally, corrosion protection of PVDF coating with modified fumed silica was evaluated by the potentiodynamic polarization test. The hydrophobic property of PVDF coating increased with the increase of HMDZ modified fumed silica. On the other hand, the hydrophobic property of PVDF coating increased when TMCS modified fumed silica is added to 30 wt%, then decreased with the increase of TMCS modified fumed silica because of formation of hydrophilic triethylammonium chloride salts. Consequently, it can be concluded that the hydrophobic

surface-modified fumed silica using HMDZ is an effective additive for improving the corrosion protection performance of the PVDF coatings.

Acknowledgments

This work was supported by a Research Grant of Pukyong National University (2019).

References

1. Y. Y. Yan, N. Gao, and W. Barthlott, *Adv. Colloid Interfac.*, **169**, 80 (2011).
2. W. Barthlott and C. Neinhuis, *Planta*, **202**, 1 (1997).
3. N. A. Patankar, *Langmuir*, **20**, 8209 (2004).
4. Y. Shi and X. Xiao, *J. Disper. Sci. Technol.*, **37**, 640 (2016).
5. R. P. S. Chakradhar, G. Prasad, P. Bera, and C. Anandan, *Appl. Surf. Sci.*, **301**, 208 (2014).
6. L. Huang, S. P. Lau, H. Y. Yang, E. S. P. Leong, S. F. Yu, and S. Prawer, *J. Phys. Chem. B*, **109**, 7746 (2005).
7. H. Liu, L. Feng, J. Zhai, L. Jiang, and D. Zhu, *Langmuir*, **20**, 5659 (2004).
8. X. Feng, L. Feng, M. Jin, J. Zhai, L. Jiang, and D. Zhu, *J. Am. Chem. Soc.*, **126**, 62 (2004).
9. D. A. Seiler, *Modern Fluoropolymers High Performance Polymers for Diverse*, pp. 1 - 637, John Wiley & Sons, New York (1997).
10. L. Yan, K. Wang, and L. Ye, *J. Mater. Sci. Lett.*, **22**, 1713 (2003).
11. C. Peng, S. Xing, Z. Yuan, J. Xiao, C. Wang, and J. Zeng, *Appl. Surf. Sci.*, **259**, 764 (2012).
12. Y. H. Kim, A study on the self cleaning effect by methyl silicate on PCM polyvinylidene fluoride coating, Pukyong National University (2013).
13. G. Wypych, *Handbook of Fillers 4th ed.*, pp. 1 - 938, ChemTec Publishing, Toronto (2016).
14. A. M. A. Mohamed, A. M. Abdullah, and N. A. Younan, *Arab. J. Chem.*, **8**, 749 (2015).
15. P. Yuan, D. Yang, Z. Lin, H. He, X. Wen, L. Wang, and F. Deng, *J. Non-Cryst. Solids*, **352**, 3762 (2006).
16. M. J. Child, M. J. Heywood, S. K. Pulton, G. A. Vicary, and G. H. Yong, *J. Colloid Interf. Sci.*, **89**, 202 (1982).
17. Adel M. A. Mohamed, Aboubakr M. Abdullah, and Nathalie A. Younan, *Arab. J. Chem.*, **8**, 749 (2015).
18. K. Sano, A. Yamada, A. Matsui, H. Tsuji, S. Hasegawa, Y. Maekawa, Effect of salt-containing filter paper attached to osmotic membrane, Desalination, **324**, 34 (2013).
19. L. Peng, W. Lei, P. Yu, and Y. Luo, *RSC Adv.*, **6**, 10365 (2016).
20. D. A. Seiler, *Modern fluoropolymers high performance polymers for diverse applications,* pp. 1 – 637, John Wiley & Sons, New York (1997).